Brain Research, 493 (1989) 331–347
Elsevier

BRES 14683

Cytoplasmic loop of β-adrenergic receptors: synaptic and intracellular localization and relation to catecholaminergic neurons in the nuclei of the solitary tracts

Chiye Aoki[1], Barbara A. Zemcik[2], Catherine D. Strader[2] and Virginia M. Pickel[1]

[1]*Division of Neurobiology, Department of Neurology, Cornell University Medical College, New York, NY 10021 (U.S.A.)* and [2]*Department of Biochemistry and Molecular Biology, Merck Sharp & Dohme Research Laboratories, Rahway, NJ 07065 (U.S.A.)*

(Accepted 10 January 1989)

Key words: β-Adrenergic receptor; Medial nucleus of the solitary tract; Membrane biogenesis; Synapse; Autonomic; Catecholamine; Autoreceptor; Immunohistochemistry; Immunoautoradiography

Pharmacological studies suggest that β-adrenergic receptors (βAR) in the medial nuclei of the solitary tracts (m-NTS) facilitate presynaptic release of catecholamines and also function at postsynaptic sites. We have localized the antigenic sites for a monoclonal antibody against a peptide corresponding to amino acids 226–239 of βAR in the m-NTS of rat brain. By light microscopy, immunoperoxidase labeling for this antibody was detected in somata and proximal processes of many small cells that were distributed throughout the rostrocaudal extent of the m-NTS. Electron microscopy confirmed the cytoplasmic localization of βAR in perikarya and proximal dendrites of neurons. Immunoreactivity occurred as discrete patches associated with cytoplasmic surfaces of plasma membrane and with irregularly-shaped saccules with clear lumen in the immediate vicinity. Select regions of nuclear envelopes, mitochondrial membranes, and rough endoplasmic reticulum were also immunoreactive along their cytoplasmic surfaces. In contrast, the Golgi apparatus was labeled, but infrequently. Immunoreactivity was also detected at numerous post- and occasional presynaptic membrane specializations of select axodendritic junctions. Dual labeling for the βAR-antibody by the immunoperoxidase method and for a rabbit antiserum against the catecholamine-synthesizing enzyme, tyrosine hydroxylase (TH), by the immunoautoradiographic method within the same sections, further established the precise cellular relations between βAR and catecholaminergic neurons. Immunoreactivity for βAR was detected in numerous perikarya and proximal dendrites that did not show detectable levels of TH. However, a few cells were dually labeled for both antigens, as seen by both light and electron microscopy. The TH-labeled terminals formed synapses at junctions both with and without βAR-like immunoreactivity. These results from the single and dual labeling studies: (1) confirm biochemical predictions that amino acids 226–239 of βAR protein reside intracellularly; (2) provide the first ultrastructural evidence for βAR localization within both pre- and postsynaptic membrane specializations of a subset of catecholaminergic synapses; and (3) suggest select intracellular sites that may be involved with synthesis and/or internalization and degradation of the receptor protein.

INTRODUCTION

The medial nuclei of the solitary tracts (m-NTS) in the medulla oblongata contain both adrenergic and noradrenergic perikarya and processes[26] as well as α- and β-adrenergic receptors (AR)[25,50,69]. Moreover, based on pharmacological evidence, Smith[58] has postulated that presynaptic β_2AR in the m-NTS may facilitate the release of norepinephrine (NE), thus partially accounting for decreases in blood pressure following local microinjections of β-adrenergic agonists. Challenges to this interpretation[15], using extracellular recording methods, point to the difficulty in determining cellular locations of receptive sites in complex and probably multisynaptic circuits of the NTS. Thus, an ultrastructural immunocytochemical approach was used in the present study to examine (1) the possible pre- vs postsynaptic localization of βAR in the NTS; and (2) their relation to catecholaminergic perikarya and terminals.

Correspondence: C. Aoki, Division of Neurobiology, Department of Neurology, Cornell University Medical College, 411 E. 69 St., New York, NY 10021, U.S.A.

We used a monoclonal antibody raised against a peptide with the sequence corresponding to amino acids 226–239 of hamster lung βAR (β_2-type). This antibody was chosen over the polyclonal antiserum against the whole βAR-protein utilized in previous studies[1,60] for the following reasons: (1) specificity of the monoclonal antibody was demonstrated by its binding to purified βAR[70] and to cloned βAR expressed in cultured cell lines[62,70] as well as by the loss of immunofluorescence paralleling down-regulation of the receptor[70]; (2) cross-reactivity of the antibody with other receptors was less likely, since the amino acid sequence of βAR's antigenic portion is unique among the G-protein-linked family of known receptors[4,7,10,16–18,27–31,36,38,39,42,67]; (3) the antibody was expected to be easily accessible to the antigenic portion of the receptor protein which, based on the commonly accepted model for the receptor's transmembrane topography, was predicted to reside within a cytoplasmic loop between the fifth and the sixth membrane-spanning helices[11,12,61,63]; and (4) dual immunolabeling with rabbit antityrosine hydroxylase (TH), an enzyme required for catecholamine synthesis, was more feasible with the mouse anti-βAR than the rabbit anti-βAR.

MATERIALS AND METHODS

Source of antibodies

The production and specificity of the monoclonal antibody against a peptide corresponding to amino acids 226–239 of hamster βAR has been described previously[70]. The antiserum to TH was produced in rabbits, characterized for its specificity[24] and generously donated to us by Dr. T.H. Joh, Div. of Molecular Biology, Dept. of Neurology, Cornell Univ. Med. Coll., New York, NY. ^{125}I-iodinated donkey anti-rabbit immunoglobulin G was commercially obtained from Amersham (Arlington Heights, IL). The avidin-biotin-peroxidase complex (ABC) kit for detection of mouse IgM was purchased from Vector Laboratories, Inc. (Burlingame, CA).

Preparation of tissue

Brains of adult male Sprague–Dawley rats were rapidly fixed under deep anesthesia (Nembutal, 50 mg/kg body wt., i.p.) by aortic arch perfusion with a mixture of acrolein and paraformaldehyde in 0.1 M phosphate buffer (pH 7.4)[37]. Coronal 40-μm Vibratome-sections containing rostral, intermediate and caudal portions of the NTS from the fixed brains were collected in phosphate buffer, then immersed in sodium borohydride (1% in phosphate buffer) for ½ h to allow for reduction reaction of residual aldehydes[13,53]. These sections were rinsed repeatedly in phosphate buffer until bubbles ceased to emerge, then preincubated in 0.1 M Tris (pH 7.6)/0.9% NaCl solution (TS) containing 0.1% bovine serum albumin.

Immunocytochemical labeling

All incubation steps were carried out at room temperature and followed by several washes with TS. *For the immunodetection of βAR*, sections were incubated overnight with culture supernatant containing the IgM monoclonal antibody, βAR(226–239)3–1, that was diluted in the range of 1:1 up to 1:100 with 0.1% bovine serum albumin/TS ±0.25% Triton X-100. Immunoreactivity was visualized within the sections of tissue using the ABC method of Hsu et al.[22].

For the simultaneous immunodetection of TH and βAR, tissue was incubated overnight with the same

→

Fig. 1. Light micrographs of the NTS labeled dually for TH and βAR. A–C: low-magnification micrographs showing the immunoperoxidase labeling (orange-brown precipitate) for βAR-like immunoreactivity together with immunoautoradiographic labeling (black grains) for TH in the m-NTS and ventrally located dorsal motor nucleus of vagus (X). The m-NTS was identified with the aid of a rat brain atlas[41] and distinguished as intermediate at the level of area postrema (B) or as rostral (A) or caudal (C) to this level. Note the dark-brown reaction for βAR in the cytoplasm of neurons with unlabeled nuclei (open arrows), to be contrasted with lighter labeling of perikarya (arrowhead) in the nucleus X. TH-immunoreactivity in perikarya, indicated by the solid arrows, also excludes the nucleus. Other black grains occur as short streaks (small double arrows) or as clusters (small single arrows). The higher-magnification micrographs in D–F show the 3 types of immunoreactive cells and processes: perikarya immunoreactive for βAR but not TH (open arrows); perikarya and processes immunoreactive for TH but not βAR (solid straight arrows and small arrows); and perikarya immunoreactive for both TH and βAR (curved solid arrows). The micrographs in D and E were taken from the intermediate m-NTS, while the micrograph in F was taken from the intermediate m-NTS corresponding to the boxed area in C. Dorso(D)-lateral(L) orientation of the sections in A–C were all as indicated in C. ts, solitary tract. Bars = 25 μm in A–C and 50 μm in D–F. Autoradiographic exposure: 4 days.

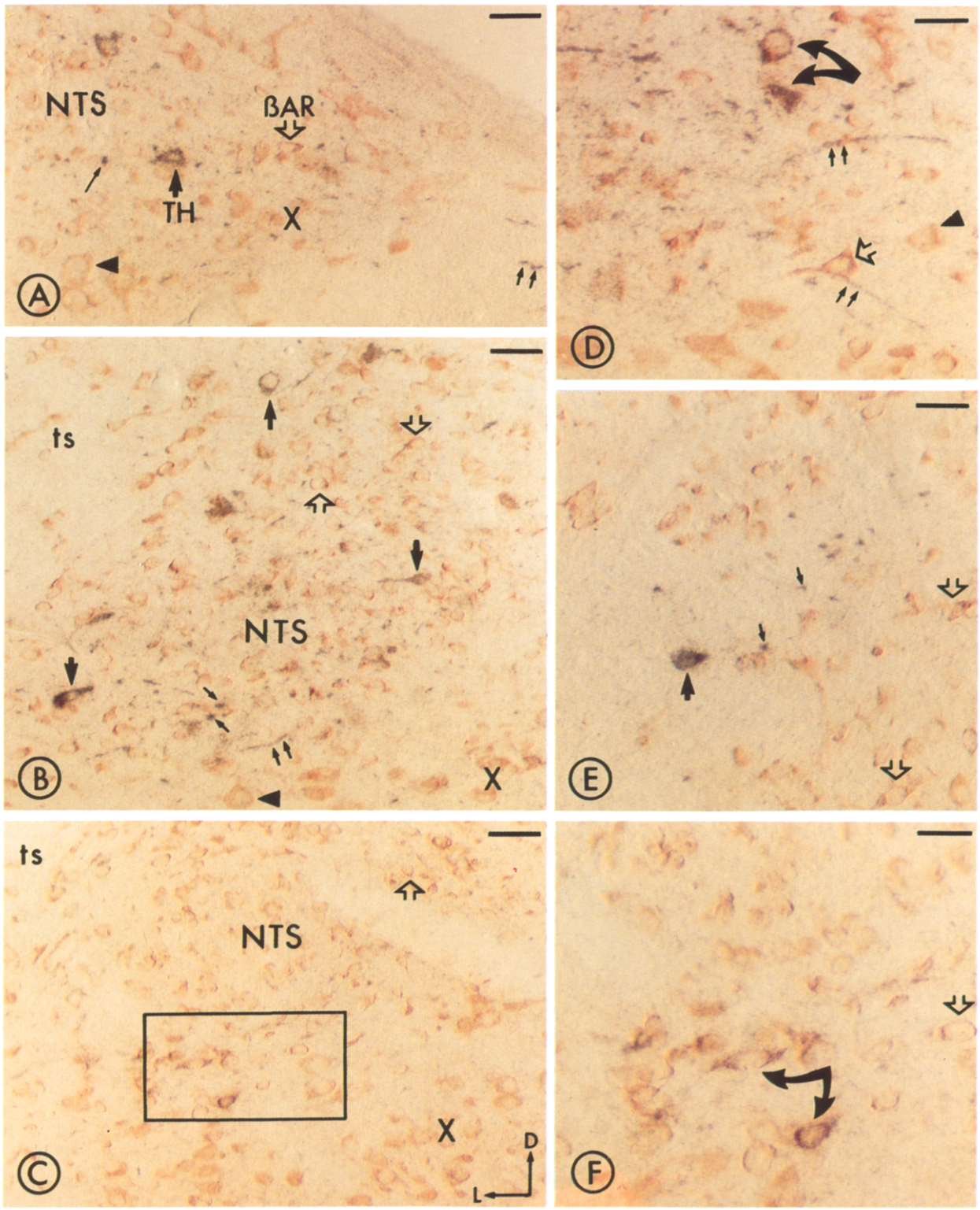
NTS
BAR
TH
X
A
ts
NTS
X
B
D
E
ts
NTS
X
D
L
C
F

antibody mixture as described above, but with the addition of rabbit anti-TH at a final dilution of 1:2000. This was followed by an incubation in ^{125}I-donkey anti-rabbit IgG at a 1:100 dilution (50 μCi/μl, 5 ml total volume) for 2 h, then the steps required for the ABC method of immunodetection.

Microscopic examination

Sections labeled by the *ABC method alone* either were mounted on glass slides and viewed by light microscopy using differential interference contrast optics or were further processed for electron microscopy[45]. Ultrathin sections were collected from the outer surface of Epon-embedded tissues. These were either (1) counterstained with uranyl acetate and lead citrate or (2) examined without counterstaining so as to facilitate the discrimination of immunoreactivity along cytoplasmic membranes and other electron-dense organelles. Tissue prepared for the *dual ABC-immunoautoradiographic labeling* were also prepared for light and electron microscopic viewing. Tissues for light microscopy were mounted on glass slides, dipped in Ilford-L4 emulsion (diluted 1:1 with distilled water at 50 °C), exposed for 4–21 days, developed with D-19 (Kodak) and viewed under differential interference contrast optics. For electron microscopy, ultrathin sections were collected from the outer surface of plastic-embedded tissue, deposited with a loop on slides coated with 2% parlodion, counterstained, carbon-coated, then dipped in Ilford-L4 emulsion (diluted 1:4 with distilled water at 50 °C). After exposure periods of 4–6 months, the autoradiographs were developed in Microdol-X (Kodak), fixed with sodium thiosulfate and transferred onto copper grids. Further details of light and electron microscopic immunoautoradiography have been described previously[44,47].

RESULTS

Light microscopic localization of βAR and TH

The light microscopic distribution of neurons showing βAR-like immunoreactivity was the same in both single and dual immunocytochemical labeling studies and, thus, is depicted only by the latter method in Fig. 1. Intense immunoperoxidase labeling was detected within the cytoplasm of numerous small (ca. 10 μm in diameter) perikarya and proximal processes of cells at the rostral, the area postrema (intermediate) and central canal (caudal) levels of the m-NTS[41] (open arrows in Figs. 1A–C). Less-intense immunoreactivity was detected within somata (arrowheads in Fig. 1A,B,D), particularly in the ventrally located dorsal motor nucleus of the vagus (X). Short, small-calibre (<0.2 μm diameter) processes with immunoreactivity were also randomly distributed between labeled perikarya. However, these processes were difficult to detect in dually-labeled sections (Fig. 1). Immunoreactivity was detectable only at dilutions of the supernatant less than 1:10. No immunoreactivity was detectable following immunocytochemical procedures using control cell culture supernatant or the dilutant alone. Membrane permeabilization, achieved by adding 0.25% Triton X-100 to the primary antibody solution, caused no apparent change in the immunostaining pattern.

TH-immunoreactive perikarya were autoradiographically detected throughout the rostrocaudal extents of NTS as well as along the dorsal border of the dorsal motor nucleus of the vagus in the same sections (solid large arrows in Fig. 1A,B,E). The perikarya often were of larger calibre (>20 μm) than the βAR-immunoreactive perikarya and were less numerous. Some of the neurons in the NTS and dorsal motor nucleus of the vagus were detectably immunoreactive both for TH and βAR (curved arrows in Fig. 1D,F). Accumulations of silver grains showing TH-immunoreactivity also occurred in round (small single arrows, Fig. 1A,B,E) and longitudinal (small double arrows, Fig. 1B,D) clusters (>50 μm in length, <0.2 μm in diameter). The size and distributions of these labeled profiles suggests that they include both dendrites and axons. The TH-labeled processes were detected near (e.g. small single arrows in Fig. 1B and E, double-arrows in Fig. 1D) as well as at a distance from perikarya and processes immunoreactive for βAR.

Ultrastructural localization of βAR-immunoreactivity

Immunolabeling for βAR in the intermediate m-NTS (at the level of the area postrema) occurred unevenly within the cytoplasm of numerous neuronal perikarya. Along perikaryal plasma membrane, labeling was discretely localized to postsynaptic sites

of some axosomatic synapses (L post in Fig. 2A), recognized by their electron density that contrasted with other unlabeled postsynaptic densities (U post in Fig. 2A). More commonly, immunoreactive plasma membrane was devoid of synaptic specializations (curved solid arrows in Fig. 2A) but, instead, closely enveloped by processes that had irregular contours and contained intermediate filament bundles characteristic of astrocytes[43]. Immunoperoxidase reaction product also occurred as clusters in the cytoplasm surrounding labeled plasma membrane. These clusters most often overlaid small saccules with clear lumen (arrowheads in Fig. 2A). The cytoplasmic surface of rough endoplasmic reticulum

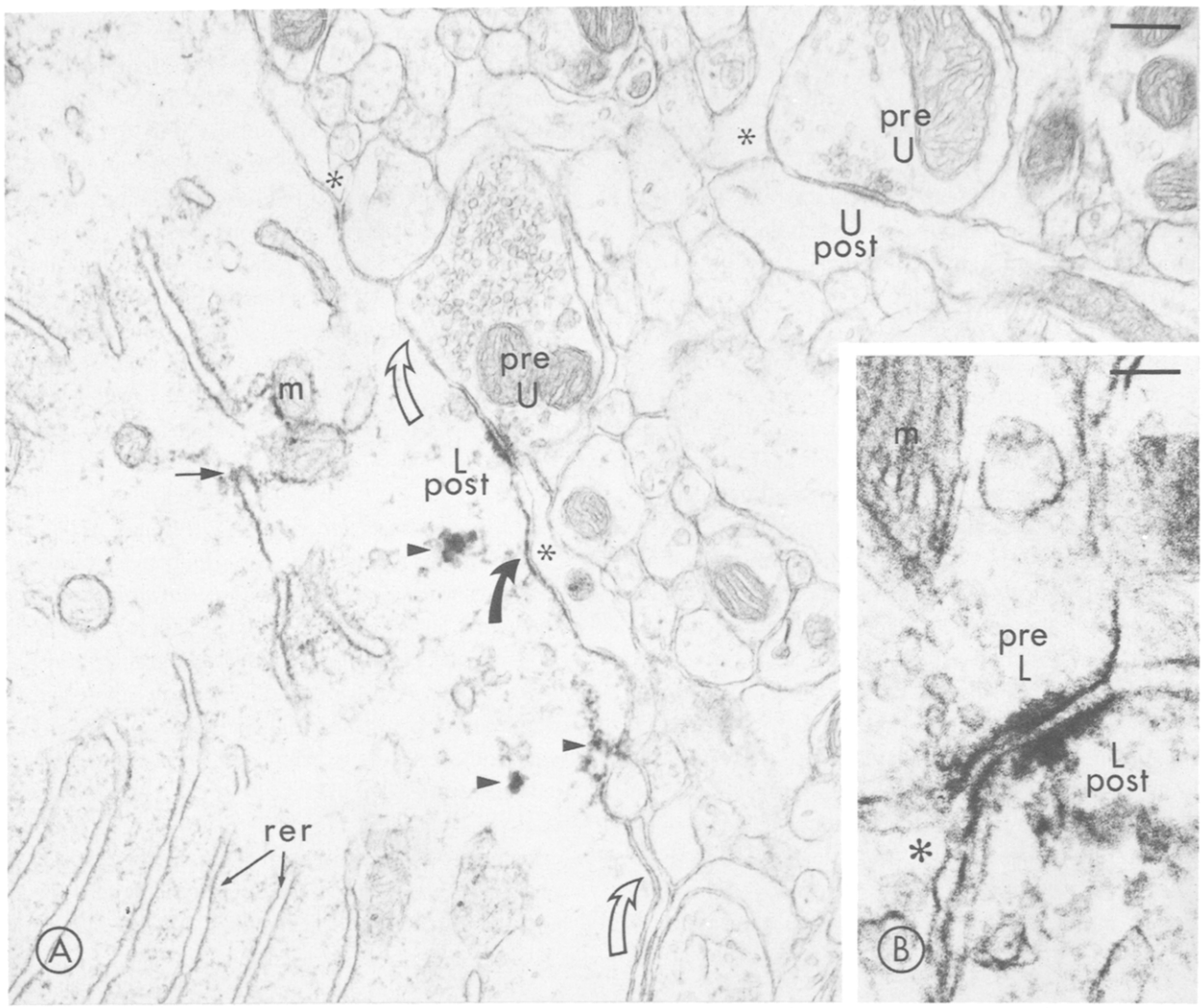

Fig. 2. Association of βAR-like immunoreactivity with synapses in the intermediate m-NTS. Electron micrograph in A shows a labeled axosomatic synapse. Immunoperoxidase reaction product is evident along portions of plasma membrane immediately postsynaptic to a cleft (L post) as well as along the plasma membrane on one side of the cleft (curved arrow) but not along the other side (open arrows). Intense immunoperoxidase reaction product also occurs as clumps in close association with small saccules near the plasma membrane (arrowheads). Less intense peroxidase reaction product is associated with certain mitochondria (m) and rough endoplasmic reticulum (small arrows) in the immediate vicinity of the labeled plasma membrane. The more organized stacks of rough endoplasmic reticulum (rer) is devoid of immunoreactivity. The presynaptic specialization (pre U) is comparable in electron-density to the unlabeled axodendritic synapse (pre U–U post). Electron micrograph in B shows labeling at both the pre- and postsynaptic membrane surfaces (pre L–L post) of an axodendritic synapse. Bars = 0.3 μm in A and 0.1 μm in B; asterisks = glial processes.

(straight arrows in Fig. 2A) and mitochondria (labeled 'm' in Fig. 2A) rarely showed detectable levels of immunoreactivity in counterstained sections.

A few dendrites and dendritic spines exhibited immunoreactivity along cytoplasmic surfaces of plasma membrane. As in perikarya, immunoreactivity along plasma membrane was not necessarily restricted to the synaptic cleft regions. At some axodendritic junctions, labeling could be detected along the cytoplasmic surfaces of both pre- and postsynaptic membranes (Fig. 2B). Labeling was excluded from extracellular synaptic-cleft regions.

The characteristic patchy labeling of intracellular and plasma membranes of neuronal perikarya and dendrites was also observed in the rostral NTS (Figs. 3–5). The discrimination of immunolabeled from non-labeled membranes was further facilitated by omitting the counterstaining steps so that the unlabeled membranes remained less electron-dense.

In perikarya, the most intensely immunoreactive aggregates of peroxidase product were detected at selective cytoplasmic regions on nuclear envelopes, plasma membrane, saccules and mitochondria (Figs. 3 and 4). Immunoreactivity was sometimes detectable for 1–2 μm along the plasma membrane which often, but not always, surrounded synaptic clefts (Fig. 3A,B). Postsynaptic densities and subjunctional bodies[40] also showed detectable levels of immunoreactivity (5 small arrows in Fig. 3A).

The central, closely stacked portions of the Golgi apparatus (the Golgi cisternae[14]) were consistently unlabeled, even when located close to intensely immunoreactive plasma membrane (Fig. 4). However, immunoreactivity was sometimes detected over peripheral Golgi vesicles (double arrow in Fig. 4B,C) and peripheral Golgi cisternae (Fig. 4B). Other, more intense aggregates of peroxidase product in unidentifiable organelles spanned the junction between the plasma membrane and peripheral Golgi cisternae. Although obscured by the immunoperoxidase product, the membranous organelles had many features of smooth endoplasmic reticulum, vesicles and saccules (Fig. 4A–C).

Discrete localization of immunoperoxidase labeling within the cytoplasm was particularly evident at axodendritic synaptic junctions found within uncounterstained ultrathin sections of the rostral NTS (Fig. 5). At the points of convergence of two axon terminals onto a dendrite, immunoreactivity was sometimes detectable over one but not the immediately adjacent postsynaptic density (Fig. 5A,C). The remaining plasma membrane also was often unlabeled. Alternatively, single axon terminals sometimes formed synaptic junctions onto two postsynaptic processes, one of which exhibited much more intense immunoreactivity than the other (Fig. 5B). Within favorable planes of section, intense immunoreactivity was also detected along small saccules which appeared to have formed either by pinocytosis of plasma membrane or by exocytosis of a vesicle (Fig. 5D).

Dual ultrastructural labeling for βAR and TH

TH-immunoreactive somata, dendrites and axon terminals were detectable within ultrathin sections from the intermediate m-NTS labeled simultaneously for TH by immunoautoradiography and for βAR by the ABC method. Electron microscopic examination confirmed light microscopic observations, indicating the existence of 3 types of neurons: immunoreactive for TH only (Fig. 6A); immunoreactive for both TH and βAR (Fig. 6B); or immunoreactive for βAR only (Fig. 6C). All sections were from the outer surface of the tissue and showed both labels within adjacent if not the same or

→

Fig. 3. The localization of βAR-like immunoreactivity within cytoplasmic rims of perikarya in the rostral NTS. Both electron micrographs were taken from uncounterstained ultrathin sections. The electron micrograph in A depicts immunoreactivity within the cytoplasm in the immediate vicinity of an axosomatic synapse (T = unlabeled axon terminal). Labeling surrounds the subjunctional body (5 small arrows) and is associated with the membranes of nearby saccules (arrowhead), the nuclear envelope (double-arrows) and portions of non-synaptic plasma membrane (curved arrow). Double-arrowhead points to a clump of immunoperoxidase reaction product that is associated with, but extends beyond, the nuclear envelope. The electron micrograph in B depicts immunoreactivity in the absence of an immunoreactive axosomatic synapse within the plane of section. Reaction product is heavily accumulated along discrete patches of the nuclear envelope (small double arrows) and appears to continue along the cytoplasmic surfaces of nearby mitochondria (m). Immunoreactivity also occurs along discrete patches of plasma membrane that are associated with immunoreactive saccules of various sizes and shapes (arrowhead). Asterisks = glial processes; curved open arrows = unlabeled plasma membrane; Cy = cytoplasm; Nu = nucleus. Bars = 0.3 μm.

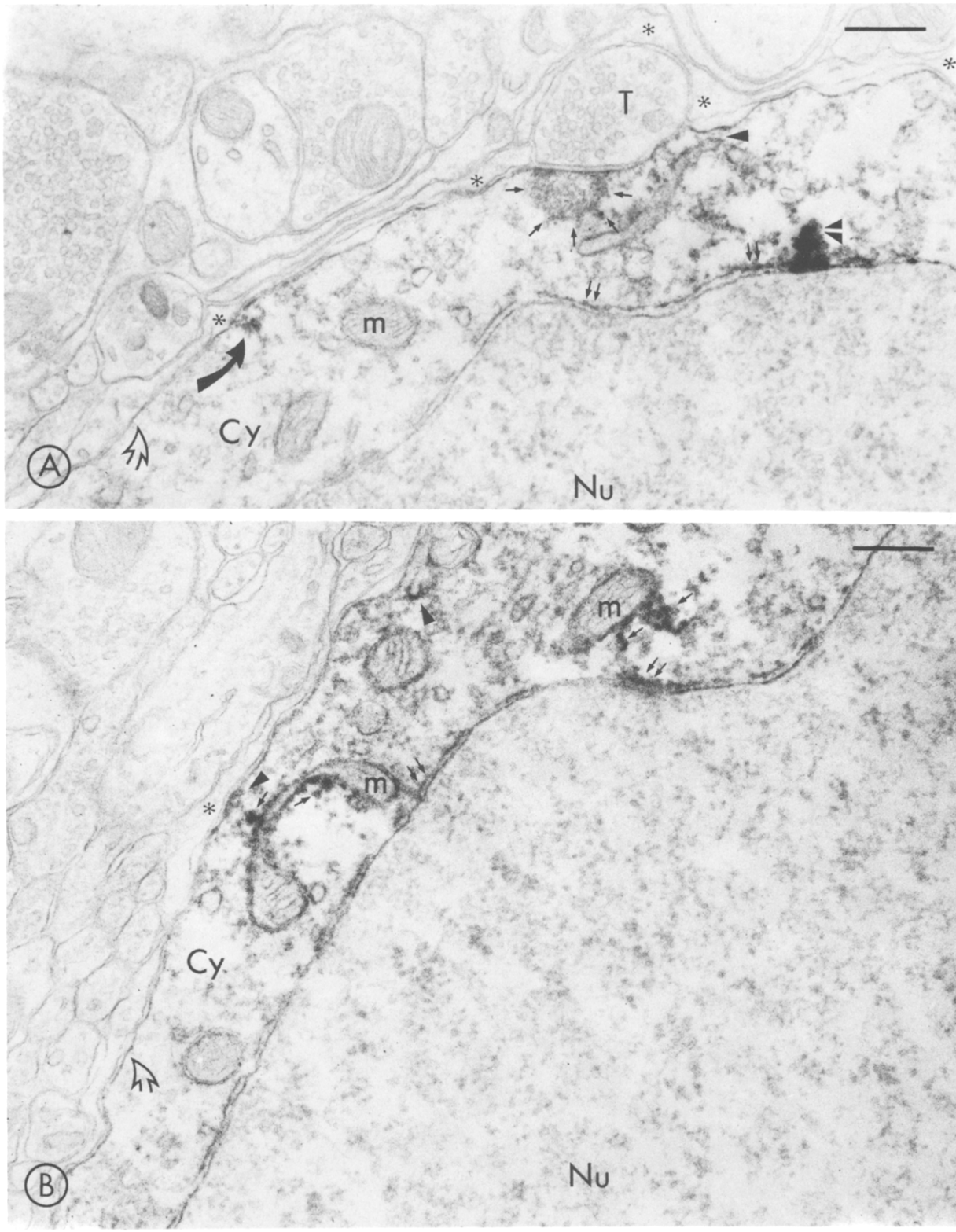
T
m
Cy
Nu
A
m
m
Cy
Nu
B

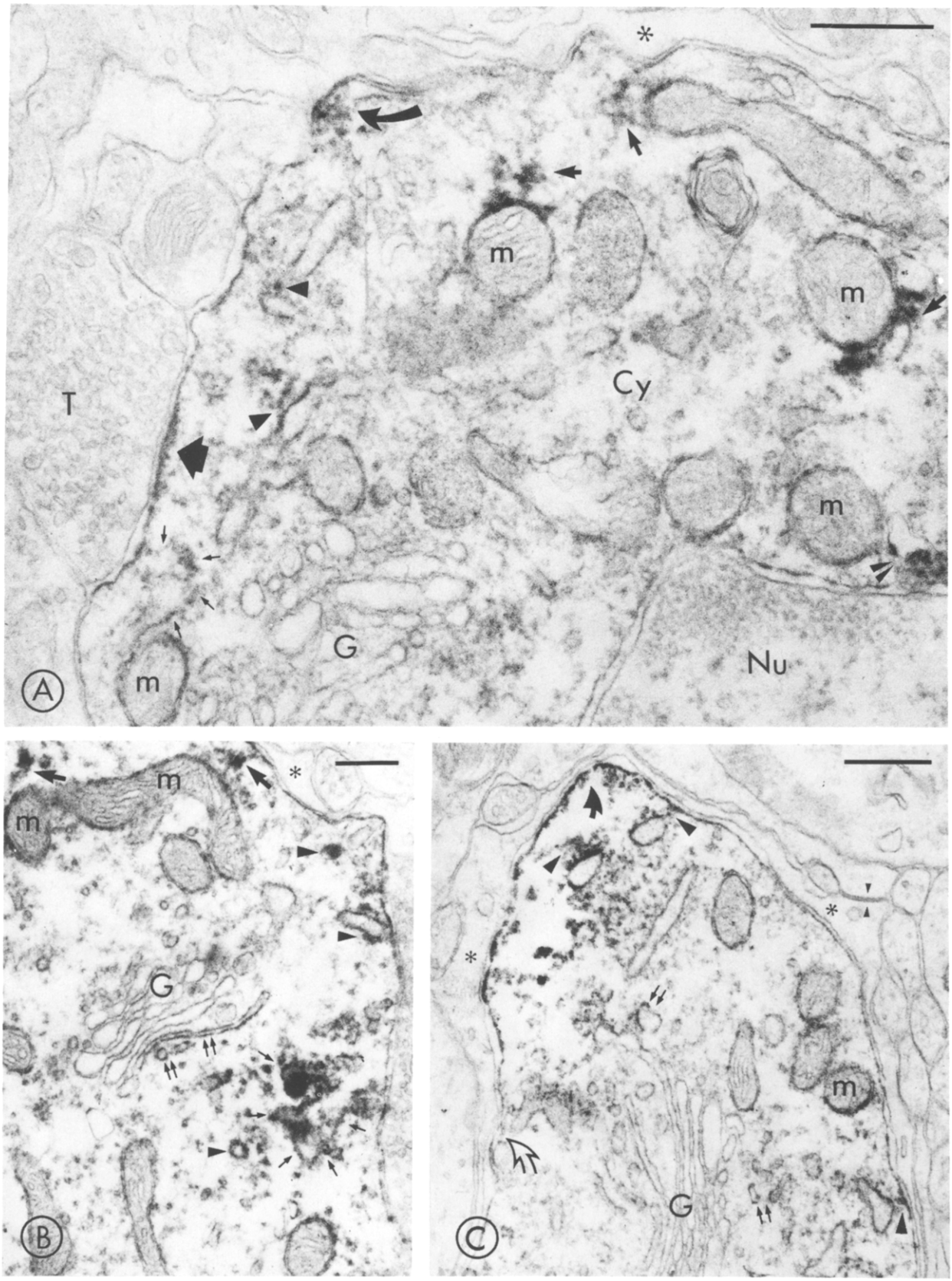
A
T
m
m
m
m
Cy
G
Nu
B
m
m
G
C
m
G

synaptically associated neurons. The βAR-like immunoreactivity was more difficult to visualize in dually labeled sections due to the overlying emulsion. Immunoreactivity was recognized largely by the greater and more electron-dense granularity in relation to other processes in surrounding neuropil. A large portion of βAR-immunoreactive perikaryal plasma membrane was devoid of association with TH-immunoreactive terminals, even though TH-terminals occurred in the immediately surrounding neuropil. (Fig. 6C).

TH-containing axons in the intermediate m-NTS occurred in at least two morphological types; those containing small, clear vesicles and the other more numerous type containing a mixture of clear and larger, dense-core vesicles (Fig. 7A). The TH-labeled terminals of both types frequently lacked synaptic specializations (Fig. 7A). Within the series of 2–4 serial sections that were examined, only a few of the junctions formed by TH-immunoreactive terminals on dendrites and dendritic spines contained βAR-immunoreactivity (Fig. 7B). The peroxidase product was distinguished from the osmiophilic reaction common to all synaptic junctions largely by comparison with unlabeled synaptic densities (Fig. 7C). Careful comparison of the synaptic densities suggested that both the pre- and postsynaptic sites may be immunoreactive for βAR. The TH-immunoreactive terminals associated with postsynaptic βAR-immunoreactivity were typically of the type containing numerous clear-round vesicles (Fig. 7B). However, TH-terminals with these morphological features also formed junctions at postsynaptic sites without βAR-immunoreactivity (Fig. 7C).

DISCUSSION

Specificity of the βAR-antibody

The amino acid sequences of many proteins known to interact with G-proteins have been recently deduced from their cDNA nucleotide sequences[17]. These sequences provide valuable information regarding the specificity of the monoclonal antibody βAR(226–239)3–1 used in the present study.The species of receptors linked to G-proteins for which the sequences are now known include visual opsins[18,38,39], β_1AR[16,67] and β_2AR[7,10,27,29], and α_2AR[28], the several subtypes of muscarinic acetylcholine receptors[4,30,31,42], the substance K receptor[36], and the mas oncogene[68]. These sequences are extensively homologous, particularly within the hydrophobic regions that are postulated to span the membrane. Homologies and conservative substitutions between the β_1- and β_2AR are also extensive (>50%) within the antigenic region corresponding to amino acids 226–239 of the hamster lung βAR. Similar comparisons between βAR and αAR indicate less homology (<25%) and virtually none with the other receptors. Based on these comparisons, we speculate that the antibody most likely recognizes one or both subtypes of the βAR, and that cross-reactivity with muscarinic and substance K receptors are probably minimal. The side-by-side association of immunoreactive and non-immunoreactive synaptic junctions with a single axon terminal is consistent with the idea that the

←

Fig. 4. Localization of βAR-immunoreactivity in portions of perikarya containing the Golgi apparatus. These electron micrographs were taken from an un-counterstained ultrathin section from the rostral m-NTS. The electron micrograph in A depicts immunoreactivity associated with cytoplasmic organelles in the vicinity of an immunoreactive axosomatic junction (large arrow). Immunoreactivity appears to be continuous towards non-synaptic regions of plasma membrane (curved arrow; asterisk = glial process) as well as along cytoplasmic saccules (arrowheads). Some of the labeled saccules span between plasma membrane and mitochondria (m) (4 small arrows in lower left and larger arrows in upper field) or are continuous with immunoreactive portions of the nuclear envelope (double arrowhead). Cisternae of the Golgi apparatus (G) are largely unlabeled. The electron micrograph in B shows a similar pattern of distribution for βAR-immunoreactivity in another perikarya in the absence of a well-defined synaptic specialization in the plane of section. βAR-immunoreactivity appears to span between the plasma membrane and an intensely immunoreactive round vesicle (5 small arrows) or irregularly shaped saccules and vesicles (arrowheads). The closely stacked central portions of the Golgi apparatus (G) are unlabeled. The reaction is seen over one Golgi vesicle and the most peripheral, flattened cisterna of the Golgi apparatus (double small arrows). Clumps of immunoreaction product are associated with mitochondria (m) (larger arrows). The electron micrograph in C shows immunoreactivity along perikaryal plasma membrane that is enveloped by glial processes (asterisks; arrowhead pair = gap junction formed between two glial processes). Near the intensely labeled portion of plasma membrane (curved arrow), immunoreactivity rims cytoplasmic saccules (arrowhead). In contrast, the Golgi apparatus (G) is non-immunoreactive except over some of the peripheral Golgi vesicles (double-arrows) close to the immunoreactive plasma membrane. Open arrow = less immunoreactive portions of plasmalemma; m = mitochondria also showing lower intensity immunoreactivity along one cytoplasmic surface. Bars = 0.3 μm.

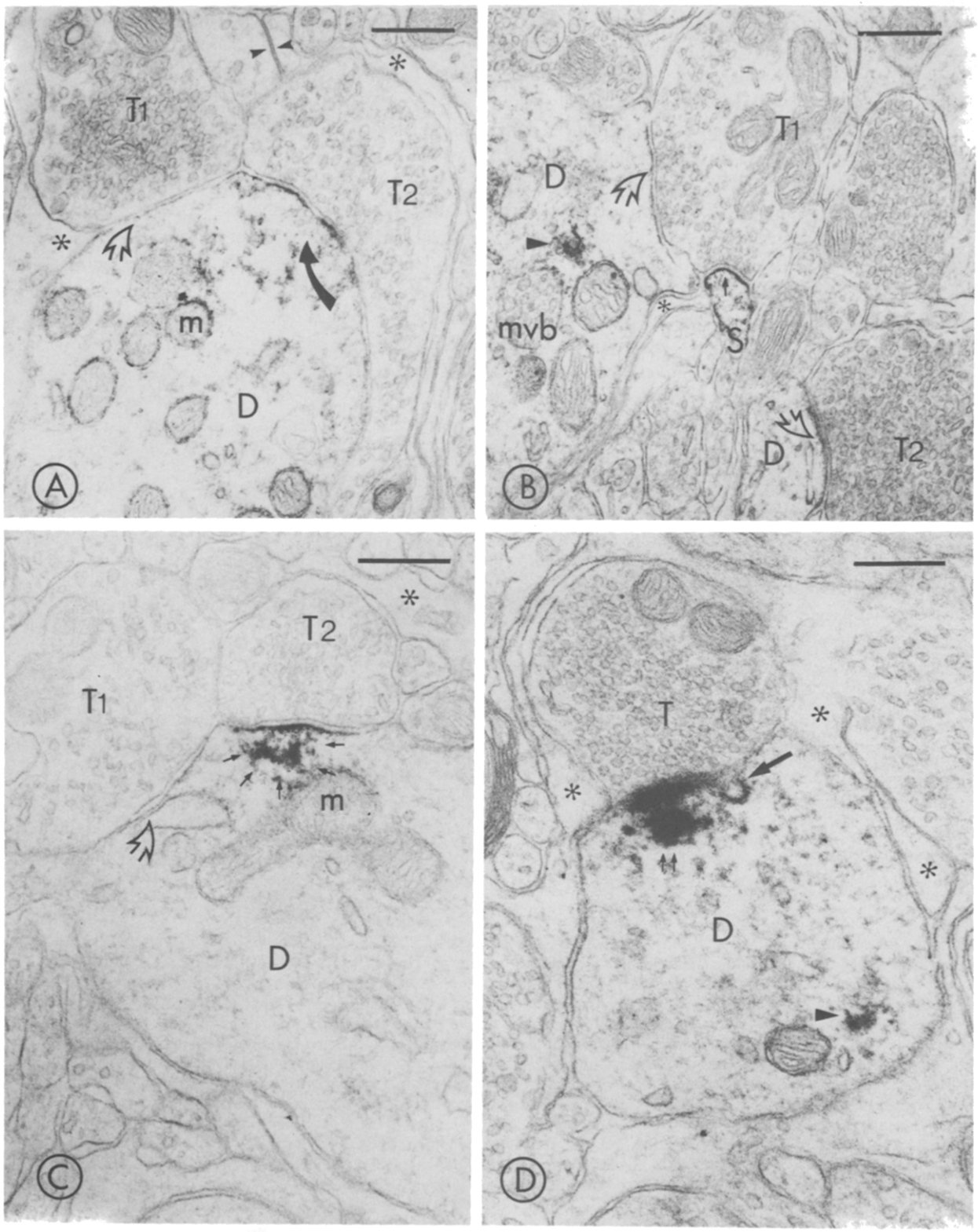
T1
T2
m
D
A
T1
D
mvb
S
D
T2
B
T2
T1
m
D
C
T
D
D

antibody recognizes one type of catecholaminergic receptor (presumably β-type) more favorably than another (presumably αAR). However, by light microscopy, we observed two levels of intensities of immunoreactivity in perikarya, the fainter of which was more widely distributed. It is possible that the less-intense immunoreactivity reflects the antibody's recognition of α-adrenergic receptors, since these are reported to occur in greater abundance in the mNTS[25,50].

Biochemical assays also point to the usefulness of the monoclonal antibody, since the antibody binds specifically to purified βAR[70], to βAR in hamster smooth-muscle DDT-1 cells[70] and in L-cells expressing the cloned βAR[62]. Further, immunofluorescence reflecting βAR/antibody-complex diminishes in parallel with the agonist-promoted down-regulation of βAR[70]. Nevertheless, the antibody still may cross-react with other G-protein-linked receptors whose amino acid sequences have yet to be determined. Such cross-reactivity could account for the widespread distribution of immunoreactivity in the NTS and dorsal motor nucleus of the vagus. Thus, the immunoreactivity should be considered as βAR-like, even if not so specified.

It should be noted that the antigen/antibody complex, although specific, probably does not form at the ligand-binding site or the G-protein-coupling site[10,12,61,63] of the receptor protein. Since immunocytochemistry using this antibody is expected to allow for detection of βAR, irrespective of its ability to bind ligands specific to βAR[70], discorrelation between immunocytochemical labeling pattern and receptor autoradiography using radioligands would be expected in the m-NTS and other brain regions.

Methodology

The ultrastructural methods used in this study were previously developed for the localization of a polyclonal rabbit antiserum against the βAR[1,60]. Under carefully controlled conditions, the immunoperoxidase method has been shown to be a reliable index for the localization of antigens to specific subcellular sites[1,48]. Difficulties such as diffusion of the diaminobenzidine reaction product appear less likely to give artifactual results, when compared to other methods that are limited by penetration (pre-embedding immunogold methods) or reductions in antigenicity due to harsh conditions used in preparation of thin plastic sections (post-embedding immunogold methods). The present and previous[1] observations of labeled and unlabeled postsynaptic densities within one dendrite attests to the feasibility of intracellular localizations using immunoperoxidase methods. One difficulty, however, in counterstained immunoperoxidase-labeled sections is the electron-density of the organelles that may be confused with the peroxidase reaction product. This difficulty is particularly evident for antigens located at membrane specializations within dually labeled sections prepared for autoradiography. We were able to recognize the βAR-like immunoreactivity in dually labeled sections only by their greater granularity and intensity in comparison to unlabeled structures within the surrounding neuropil. Comparative examinations of counterstained and uncounterstained material confirmed our ability to adequately discriminate immunolabeled from unlabeled organelles. However, it is most probable that we have failed to detect low levels of immunoreactivity over some of the electron-dense organelles.

←

Fig. 5. Synaptic specificity in βAR-like immunoreactivity. Electron micrographs A–D were taken from un-counterstained sections of the rostral m-NTS. In A the portion of plasmalemma postsynaptic to terminal 2 (T2) is intensely immunoreactive (curved arrow), while the plasma membrane postsynaptic to terminal 1 (T1) is unlabeled (open arrow). Arrowhead pair = gap junction formed between two glial processes. In B, plasma membrane of a dendritic spine (S) is most immunoreactive in the portion postsynaptic to terminal 1 (T1). In contrast, the postsynaptic density of a dendrite (D) postsynaptic to the same terminal is much less immunoreactive (open arrow), even though some of its cytoplasmic organelles are weakly immunoreactive (arrowhead). Postsynaptic density associated with another terminal (T2) is weakly immunoreactive (open arrow). mvb = multivesicular body. In C, the immunoreactivity appears to conform to the structures of postsynaptic densities (along the postsynaptic membrane) and subjunctional bodies (5 small arrows) associated with terminal 2 (T2) but not terminal 1 (T1) (open arrow of a proximal dendrite, D). Electron micrograph in D depicts immunoreactivity associated with a synaptic junction as well as the cytoplasmic organelle in the vicinity of subjunctional body (small double arrows). The reaction also extends along the postsynaptic membrane with acute curvature resembling a pinocytotic or exocytotic vesicle (larger arrow). The rest of the dendritic cytoplasm (D) exhibits little immunoreactivity except for a small aggregate at the opposite pole from the synaptic junction (arrowhead). The cytoplasm of presynaptic terminal (T) is not labeled. Asterisks = glial process; m = mitochondria; bars = 0.3 μm.

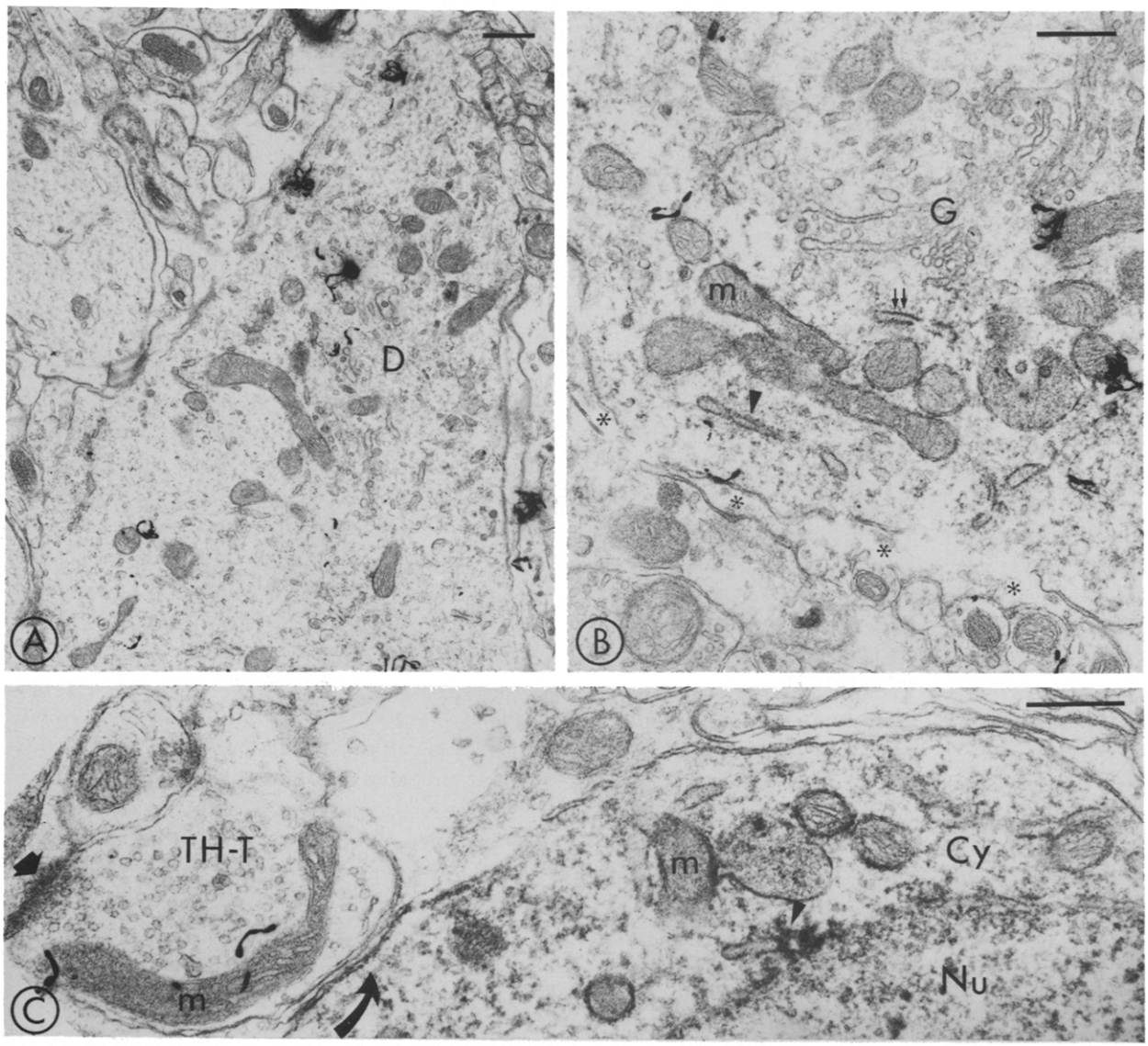

Fig. 6. Dual localization TH and βAR in neurons of the m-NTS. The electron microscopic autoradiograph in A shows TH-immunoreactivity (black squiggles = silver grains) within a proximal dendrite (D) in the absence of βAR-immunoreactivity. The autoradiograph in B shows perikarya of another neuron exhibiting immunoreactivity both for βAR along peripheral saccules (small double arrows) of Golgi apparatus (G) and rough endoplasmic reticulum near plasma membrane (arrowhead) and for TH (silver grains). The boundary of this portion of the perikarya is delimited by a glial process (asterisks). The autoradiograph in C depicts the lack of synaptic association between a TH-containing terminal (TH-T; flat arrow points to its associated synaptic junction) and a βAR-immunoreactive perikarya. Curved arrow and arrowhead point to immunoreactive portions of plasma membrane and nuclear envelope, respectively. Cy = cytoplasm; Nu = nucleus; m = mitochondria. Bars = 0.5 μm. Autoradiographic exposure = 4 months.

Light microscopic distribution and general morphological features

The abundant light microscopic distribution and small perikaryal size of neurons immunoreactive for βAR are comparable to those containing GABA in the intermediate m-NTS.[49] GABAergic neurons in the caudal NTS also share ultrastructural features in common with βAR-immunoreactive somata: a thin rim of cytoplasm, relatively few somatic contacts and a highly indented nuclear envelope[49]. These GABAergic neurons receive direct synaptic input from phenylethanolamine *N*-methyltransferase (PNMT)-

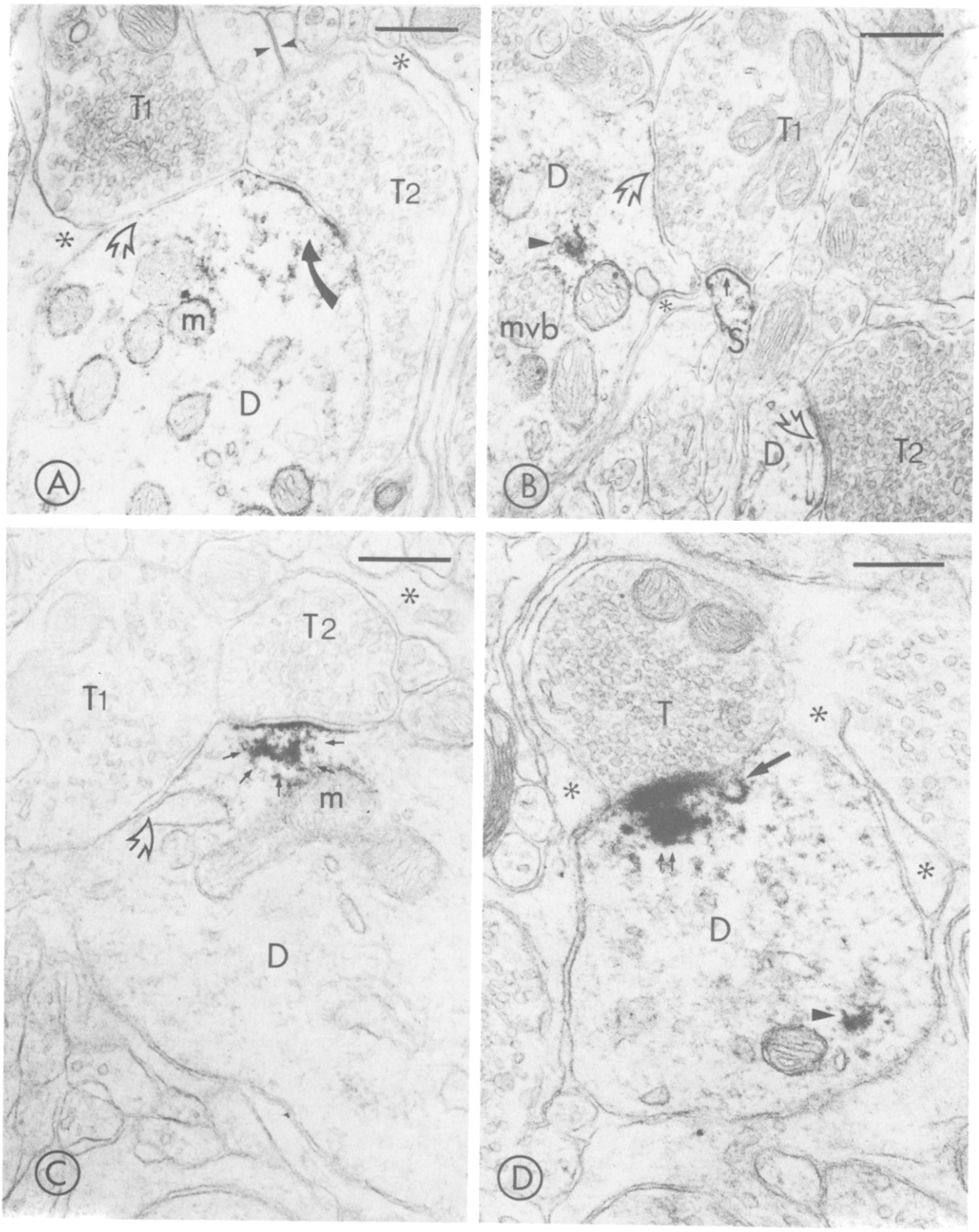

caudal[26,46,51] NTS may be adrenergic. Specifically, in the caudal NTS, the perikarya have features similar to those containing PNMT[49]. The presence of both βAR and catecholamine enzymes,[56] since many of the large TH-labeled neurons of the A2 group contained no detectable βAR-like immunoreactivity.

Additionally, many cells were immunolabeled for βAR, but lacked TH-immunoreactivity. Further dual labeling studies are needed to establish whether the βAR-containing neurons also contain GABA, PNMT or other transmitters.

Subcellular localization

The sidedness of the ultrastructural immunolabeling observed in these preparations provides the first direct morphological support for predictions based on amino acid sequences[10,12,18,60,61,70] that the antigenic portion of βAR resides on cytoplasmic surfaces of plasma membrane. The cytosolic site for antibody recognition also serves to explain the apparent lack of change in light microscopic immunostaining following detergent permeabilizations, since only antibody accessibility to any *intra*-membrane region of the protein would be expected to be enhanced by this step.

The results demonstrate that a significant portion of the βAR occurs in intracellular regions that are separate, but in close proximity to immunoreactive plasma membrane. This observation is consistent with previous reports for intracellular (i.e. also non-synaptic) acetylcholine receptors and α-subunits of voltage-dependent sodium channel, both of which have been estimated to consist of as much as two-thirds of the entire population[23,55,59].

Prominent immunoreactivity was associated with cytoplasmic surfaces of clear-lumen saccules near plasma membrane, with postsynaptic membranes that were fusing with vesicles and in the peripheral portions of the Golgi apparatus. These cytoplasmic organelles are intimately involved in the biosynthesis, endocytosis and recycling of membranes[14]. Thus, the observed immunolabeling pattern is consistent with currently accepted intracellular mechanisms involved in agonist-stimulated internalization and degradation of βAR[5,6,57,70]. Alternatively, the immunoreactivity may be attributable to newly synthesized pools of βAR yet to be incorporated into plasma membrane. If this is the case, it is unclear why larger portions of the Golgi apparatus were not immunoreactive. Reports on protein biosynthesis suggest that the period required for protein glycosylation within the Golgi apparatus is relatively short compared to the translational step at rough endoplasmic reticulum or transport and storage within vacuoles and vesicles[14]. Therefore, immunodetectability within the Golgi apparatus may possibly be more difficult, due to the smaller fraction of βAR residing in this state.

Granular aggregates of peroxidase product were discretely associated with cytoplasmic surfaces of mitochondria, usually in the vicinity of βAR-immunoreactive plasma membrane or nuclear envelopes. This immunolabeling pattern may reflect intracellular binding sites for catecholaminergic metabolism, such as oxidative degradation, a process that is catalyzed by monoamine oxidases in outer mitochondrial membranes[65]. Alternatively, the labeling may reflect the origin of mitochondrial membrane and plasmalemma from the common pool of cellular membrane[3,66]. Artifactual labeling of mitochondria by diffusion of the diaminobenzidine product, as seen with more soluble antigens such as TH[45], seems less likely due to the aggregated distribution and selectivity of the localization.

The postsynaptic localization of immunoreactivity detected at select junctions is consistent with earlier studies using a polyclonal antiserum against βAR in the striatum, cortex and cerebellum[1,60]. However, the present labeling is the first to demonstrate that, at some junctions, both pre- and postsynaptic sites show βAR-like immunoreactivity. This may be due to greater accessibility of the antibodies to antigens or, possibly, regional variations in terms of the relative prevalence of presynaptic βAR. Even in the NTS, the presynaptic sites were infrequently detected in comparison to postsynaptic sites (<0.5%). It is unlikely that the presynaptic immunolabeling is caused by the diffusion of immunoperoxidase product, since within favorable planes of section, the synaptic cleft was clearly devoid of labeling. The absence of immunoreactivity in other portions of the axon contrasts the observations in dendrites. It is possible that βAR undergo conformational changes following post-translational modification in such a way as to render the cytoplasmic loop(s) non-antigenic or not accessible to the immunolabeling solutions during axonal transport.

In dually labeled sections from the m-NTS, TH-immunoreactive axon terminals and βAR-immunoreactive postsynaptic sites usually were not aligned. Almost half of the PNMT-containing (adrenergic) and TH-containing (catecholaminergic)

terminals fail to show membrane specializations within single or small series (2–4) sections (ref. 49 and present observations). Fewer still of these membrane specializations exhibited βAR-immunoreactivity. Conversely, not all βAR-immunoreactivity was associated with detectable levels of TH in presynaptic terminals. By analogy to the extrajunctional, newly synthesized acetylcholine receptors at neuromuscular junctions[54], βAR-immunoreactivity observed along non-synaptic plasma membrane may reflect the extra-synaptic receptor proteins yet to undergo anchoring within the cleft. These receptor proteins recognized by the monoclonal antibody may or may not exhibit selective ligand-binding characteristics that would be recognized by receptor autoradiography. Alternatively, non-synaptic localizations of immunoreactivity along plasma membrane may be interpreted as the receptive sites for norepinephrine that are released at distances greater than that defined by synaptic clefts. Such non-synaptic release and 'non-classical' synapses have previously been suggested for many neurotransmitters and neuromodulators, including the catecholamines[2,9,19,34]. The non-TH-immunoreactive terminals cannot unequivocally be characterized as non-catecholaminergic, since detections using immunoautoradiography (for TH) are more limited than the ABC method. Additionally, βAR was difficult to detect in distal dendrites, the most common synaptic sites for TH-immunoreactive terminals. Possibilities also remain that the catecholaminergic terminals presynaptic to βAR-immunoreactive sites reside outside the plane of ultrathin sections. Finally, the apparent mismatch between TH-containing terminals and βAR-immunoreactive sites may reflect cross-reactions of the antibody with non-catecholaminergic receptor proteins or other non-receptor proteins. Future studies that systematically quantitate the spatial relations of catecholaminergic axon terminals and βAR by dual ultrastructural immunocytochemistry are needed.

The function of βAR in cardiovascular control

The present localization of βAR at pre- and postsynaptic sites within the cardiovascular portions of the m-NTS (intermediate level) supports pharmacological evidence implicating a role for βAR with changes in blood pressure elicited by microinjections of catecholamines directly into the solitary tract nuclei[58]. However, the most well-documented hypotensive actions of norepinephrine and its agonists are mediated by α_2AR[8,15,58]. Since the cells immunolabeled for βAR in the present study were primarily small, Feldman and Moise's failure to detect a βAR-mediated inhibition of neuronal firing in the m-NTS[15] may, at least partially, have been due to their electrophysiological recording conditions that selected for large neurons. Also, unlike the αAR, the βAR is activated by low tonic levels of released catecholamines[58] and rapidly becomes desensitized[35,64] following elevated levels of its release[32,33]. Thus desensitization might account for failure of βAR-antagonists to alter the firing of neurons in the m-NTS following iontophoretic applications of amines[15]. Since elevations of catecholamines are also seen in the m-NTS of certain strains of hypertensive rats[21,52], the role of βAR desensitization in the etiology of central neurogenic hypertension seems worthy of more extensive investigation.

REFERENCES

1 Aoki, C., Joh. T.H. and Pickel, V.M., Ultrastructural localization of β-adrenergic receptor-like immunoreactivity in the cortex and neostriatum of rat brain, *Brain Research,* 437 (1987) 264–282.

2 Beaudet, A. and Descarries, L., The monoamine innervation of rat cerebral cortex: synaptic and non-synaptic axon terminals, *Neuroscience,* 3 (1978) 851–860.

3 Blok, M.C., Wirtz, K.W.A. and Scherphof, G.L., Exchange of phospholipids between microsomes and inner and outer membranes of rat liver, *Biochim. Biophys. Acta,* 233 (1971) 61–75.

4 Bonner, T.I., Buckley, N.J., Young, A.C. and Brann, M.R., Identification of a family of muscarinic acetylcholine receptor genes, *Science,* 237 (1987) 527–532.

5 Chuang, D.M. and Costa, E., Evidence for internalization of the recognition site of β-adrenergic receptors during receptor subsensitivity induced by (−)-isoproterenol, *Proc. Natl. Acad. Sci. U.S.A.,* 76 (1979) 3024–3028.

6 Chuang, D.M., Dillon-Carter, O., Spain, J.W., Laskowski, M.B., Roth, B.L. and Coscia, C.J., Detection and characterization of β-adrenergic receptors and adenylate cyclase in coated vesicles isolated from bovine brain, *J. Neurosci.,* 6 (1986) 2578–2584.

7 Chung, F.Z. Lentes, K.-U., Gocayne, J., Fitzgerald, M., Robinson, D., Kerlavage, A.R., Fraser, C.M. and Venter, J.C., Cloning and sequence analysis of the human brain β-adrenergic receptor, *FEBS Lett.,* 211 (1987) 200–206.

8 DeJong, W. and Petty, M., Chemical stimulation of the

nucleus of the solitary tract and the resulting blood pressure response. *J. Cardiovasc. Pharmacol.*, 4, Suppl. 1 (1982) 577–580.
9 Descarries, L., Watkins, K.C. and Lapierre, Y., Noradrenergic axon terminals in the cerebral cortex of rat. III. Topometric ultrastructural analysis, *Brain Research*, 133 (1977) 197–222.
10 Dixon, R.A.F., Kobilka, B.K., Strader, D.J., Benovic, J.L., Dohlman, H.G., Frielle, T., Bolanowski, M.A., Bennett, C.D., Rands, E., Diehl, R.E., Mumford, R.A., Slater, E.E., Sigal, I.S., Caron, M.G., Lefkowitz, R.J. and Strader, C.D., Cloning of the gene and cDNA for mammalian β-adrenergic receptor and homology with rhodopsin, *Nature (Lond.)*, 321 (1986) 75–79.
11 Dixon, R.A.F., Sigal, I.S., Irving S., Rands, E., Register, R.B., Candelore, M.R., Blake, A.D. and Strader, C.D., Ligand binding to the β-adrenergic receptor involves its rhodopsin-like core, *Nature (Lond.)*, 326 (1987) 73–77.
12 Dixon, R.A.F., Sigal, I.S., Candelore, M.R., Register, R.B., Scattergood, W., Rands, E. and Strader, C.D., Structural features required for ligand binding to the β-adrenergic receptor, *EMBO J.*, 6 (1987) 3269–3275. (1987).
13 Eldred, W.D., Zucker, C., Karten, H.J. and Yazula, S. Comparison of fixation and penetration enhancement techniques for use in ultrastructural immunocytochemistry, *J. Histochem. Cytochem.*, 31 (1983) 285–292.
14 Farquar, M.G., Progress in unraveling pathways of Golgi traffic, *Ann. Rev. Cell Biol.*, 1 (1985) 447–488.
15 Feldman, P.D. and Moises, H.C., Adrenergic responses of baroreceptive cells in the nucleus tractus solitarii of the rat: a microiontophoretic study, *Brain Research*, 420 (1987) 351–361.
16 Frielle, T., Collins, S., Daniel, K.W., Caron, M.G., Lefkowitz, R.J. and Kobilka, B.K., Cloning of the cDNA for the human β_1-adrenergic receptor, *Proc. Natl. Acad. Sci U.S.A.*, 84 (1987) 7920–7924.
17 Hanley, M.R. and Jackson, T., Return of the magnificent seven, *Nature (Lond.)*, 329 (1987) 766–767.
18 Hargrave, P.A., McDowell, J.H., Feldmann, R.J., Atkinson, P.H., Rao, J.K.M. and Argos, P., Rhodopsin's protein and carbohydrate structure: selected aspects, *Vision Res.*, 24 (1984) 1487–1499.
19 Herkenham, M., Mismatches between neurotransmitter and receptor localizations in brain: observations and implications, *Neuroscience*, 23 (1987) 1–38.
20 Hökfelt, T., Fuxe, K., Goldstein, M. and Johansson, O., Immunohistochemical evidence for the existence of adrenaline neurons in the rat brain, *Brain Research*, 66 (1974) 235–251.
21 Howe, P.R.C., Lovenberg, W. and Chalmers, J.P., Increased number of PNMT-immunofluorescent nerve cell bodies in the medulla oblongata of stroke-prone hypertensive rats, *Brain Research*, 205 (1981) 123–130.
22 Hsu, S.M., Raine, L. and Fanger, H., Use of avidin-biotin-peroxidase complex (ABC) in immunoperoxidase techniques: a comparison between ABC and unlabeled antibody (PAP) procedures, *J. Histochem. Cytochem.*, 29 (1981) 577–580.
23 Jacob, M.H., Lindstrom, J.M. and Berg, D.K., Surface and intracellular distribution of a putative neuronal nicotinic acetylcholine receptor, *J. Cell Biol.*, 103 (1986) 205–214.
24 Joh. T.H., Gegham, C. and Reis, D.J., Immunochemical demonstration of increased tyrosine hydroxylase protein in sympathetic ganglia and adrenal medulla elicited by reserpine, *Proc. Natl. Acad. Sci. U.S.A.*, 70 (1973) 2767–2771.
25 Jones, L.S., Gauger, L.L. and Davis, J.N., Anatomy of brain alpha$_1$-adrenergic receptors: in vitro autoradiography with [^{125}I]Heat, *J. Comp. Neurol.*, 231 (1985) 190–208.
26 Kalia, M. and Fuxe, K., Rat medulla oblongata. II. Dopaminergic, noradrenergic (A1 and A2) and adrenergic neurons, nerve fibers and presumptive terminal processes, *J. Comp. Neurol.*, 233 (1985) 308–332.
27 Kobilka, B.K., Dixon, R.A.F., Frielle, T., Dohlman, H.G., Bolanowski, M.A., Sigal, I.S., Yang-Feng, T.L., Francke, U., Caron, M.G. and Lefkowitz, R.J., cDNA for the human β_2-adrenergic receptor: a protein with multiple membrane-spanning domains and encoded by a gene whose chromosomal location is shared with that of the receptor for platelet-derived growth factor, *Proc. Natl. Acad. Sci. U.S.A.*, 83 (1987) 46–50.
28 Kobilka, B.K., Matsui, H., Kobilka, T.S., Yang-Feng, T.L., Francke, U., Caron, M.G., Lefkowitz, R.J. and Regan, J.W., Cloning, sequencing and expression of the gene coding for the human platelet α_2-adrenergic receptor, *Science*, 238 (1987) 650–656.
29 Kobilka, B.K., Frielle, T., Dohlman, H.G., Bolanowski, M.A., Dixon, R.A.F., Keller, P., Caron, M.G. and Lefkowitz, R.J., Delineation of the intronless nature of the genes for the human and hamster β_2-adrenergic receptor and their putative promotor regions, *J. Biol. Chem.*, 262 (1987) 7321–7327.
30 Kubo, T., Primary structure of porcine cardiac muscarinic acetylcholine receptor deduced from the cDNA sequence, *FEBS Lett.*, 209 (1986) 367–372.
31 Kubo, T., Fukuda, K., Mikami, A., Maeda, A., Takahashi, H., Mishina, M., Haga, T., Haga, K., Ichiyama, A., Kangawa, K., Kojima, M., Matsuo, H., Hirose, T. and Numa, S., Cloning, sequencing and expression of cDNA encoding the muscarinic acetylcholine receptor, *Nature (Lond.)*, 323 (1986) 411–416.
32 Kvetnansky, R., Saavedra, J.M. and Kopin, I.J., Changes in epinephrine in individual hypothalamic nuclei after immobilization stress, *Brain Research*, 155 (1978) 387–390.
33 Lefkowitz, R.J., Mini review: the β-adrenergic receptor, *Life Sci.*, 18 (1976) 461–472.
34 Libet, B., Non-classical synaptic functions of transmitters, *Fed. Proc. Fed. Am. Soc. Exp. Biol.*, 45 (1986) 2678–2686.
35 Maggi, A., U'Pritchard, D.C. and Enna, S.J., β-adrenergic regulation of α_2-adrenergic receptors in the central nervous system, *Science*, 207 (1980) 645–647.
36 Masu, Y., Nakayama, K., Tamaki, H., Harada, Y., Kuno, M. and Nakanishi, S., cDNA cloning of bovine substance-k receptor through oocyte expression system, *Nature (Lond.)*, 329 (1987) 836–840.
37 Milner, T.A., Pickel, V.M., Park, D.H., Joh, T.H. and Reis, D.J., Phenylethanolamine *N*-methyltransferase-containing neurons in the rostral ventrolateral medulla of the rat. I. Normal ultrastructure, *Brain Research*, 411 (1987) 28–45.
38 Nathans, J. and Hogness, D.S., Isolation, sequence analysis, and intron-exon arrangement of the gene encoding bovine rhodopsin, *Cell*, 34 (1983) 807–814.
39 Nathans, J., Thomas, D. and Hogness, D.S., Molecular genetics of human color vision: the genes encoding blue, green, and red pigments, *Science*, 232 (1986) 193–202.
40 Pappas, G.D. and Waxman, S.G., Synaptic fine structure–

morphological correlates of chemical and electrotonic transmission. In G.D. Pappas and D.P. Purpura (Eds.), *Structure and Function of Synapses,* Raven, New York, 1972, pp. 1–43.

41 Paxinos, G. and Watson, C., *The Rat Brain in Stereotaxic Coordinates,* 2nd. edn., Academic, New York, 1986.

42 Peralta, E.G., Winslow, J.W., Peterson, G.L., Smith, D.H., Ashkenazi, A., Ramachandran, J., Schimerlik, M.I. and Capon, D.J., Primary structure and biochemical properties of an M_2 muscarinic receptor, *Science,* 236 (1987) 600–605.

43 Peters, A., Palay, S.L. and Webster, H., *The Fine Structure of the Nervous System: The Neurons and Supporting Cells,* Sanders, Philadelphia, 1976, 90 pp.

44 Pickel, V.M. and Beaudet, A., Combined use of autoradiography and immunocytochemical methods to show synaptic interactions between chemically defined neurons. In J.M. Polak and I.M. Varndell (Eds.), *Immunolabeling for Electron Microscopy,* Elsevier, Amsterdam, 1984, pp. 259–265.

45 Pickel, V.M., Beckley, S.C., Joh, T.H. and Reis, D.J., Ultrastructural immunocytochemical localization of tyrosine hydroxylase in neostriatum, *Brain Research,* 225 (1981) 373–385.

46 Pickel, V.M., Chan, J., Park, D.H., Joh, T.H. and Milner, T.A., Ultrastructural localization of phenylethanolamine *N*-methyltransferase in sensory and motor nuclei of the vagus nerve, *J. Neurosci. Res.,* 15 (1986) 439–455.

47 Pickel, V.M., Chan, J. and Milner, T.A., Autoradiographic detection of ^{125}I-secondary antiserum: a sensitive light and electron microscopic method compatible with peroxidase immunocytochemistry for dual localization of neuronal antigens, *J. Histochem. Cytochem.,* 34 (1986) 707–718.

48 Pickel, V.M., Chan, J. and Massari, V.J., Neuropeptide Y-like immunoreactivity in neurons of the solitary tract nuclei: vesicular localization and synaptic input from GABAergic terminals, *Brain Research,* 476 (1989) 265–278.

49 Pickel, V.M., Chan, J. and Milner, T.A., Cellular substrates for interactions between neurons containing phenylethanolamine *N*-methyltransferase and GABA in the nuclei of the solitary tracts, *J. Comp. Neurol.,* in press.

50 Rainbow, T.C., Parson, B. and Wolfe, B.B., Quantitative autoradiography of β_1- and β_2-adrenergic receptors in rat brain, *Proc. Natl. Acad. Sci. U.S.A.,* 81 (1984): 1585–1589.

51 Ruggiero, D.A., Ross, C.A., Anwar, M., Park, D.H., Joh, T.H. and Reis, D.J., Distribution of neurons containing phenylethanolamine *N*-methyltransferase in medulla and hypothalamus of rat, *J. Comp. Neurol.,* 239 (1985) 127–154.

52 Saavedra, J.M., Grobecker, H., Axelrod, J., Changes in central catecholaminergic neurons in the spontaneously (genetic) hypertensive rat, *Circ. Res.,* 42 (1978) 529–533.

53 Schachner, M., Hedley-Whyte, E.T., Hsu, D.W., Schoonmaker, G. and Bignami, A., Ultrastructural localization of glial fibrillary acidic protein in mouse cerebellum by immunoperoxidase labeling, *J. Cell Biol.,* 75 (1977) 67–73.

54 Scheutze, S.M. and Role, L.W., Developmental regulation of nicotinic acetylcholine receptors, *Ann. Rev. Neurosci.,* 10 (1987) 403–457.

55 Schmidt, J., Rossie, S. and Catterall, W.A., A large intracellular pool of inactive Na channel α subunits in developing rat brain, *Proc. Natl. Acad. Sci. U.S.A.,* 82 (1985) 4847–4851.

56 Shorr, R.G.L., Minnich, M.D., Varrichio, A., Strohsacker, M.W., Gotlib, L., Kruse, L.I., DeWolf, W.E. and Crooke, S.T., Immuno cross-reactivity suggests that catecholamine biosynthesis enzymes and β-adrenergic receptors may be related, *Mol. Pharmacol.,* 32 (1987) 195–200.

57 Sibley, D.R. and Lefkowitz, R.J., Molecular mechanisms of receptor desensitization using the β-adrenergic receptor-coupled adenylate cyclase system as a model, *Nature (Lond.),* 317 (1985) 125–129.

58 Smith, W.L., Egle Jr., J.L. and Adams, M.D., Adrenergic receptors in the nucleus tractus solitarii of the rat, *Eur. J. Pharmacol.,* 81 (1982) 11–19.

59 Stollberg, J. and Berg, D.K., Neuronal acetylcholine receptors: fate of surface and internal pools in cell culture, *J. Neurosci.,* 7 (1987) 1809–1815.

60 Strader, C.D., Pickel, V.M., Joh, T.H., Strohsacker, M.W., Shorr, R.G.L., Lefkowitz, R.J. and Caron, M.C., Antibodies to the β-adrenergic receptor: attenuation of catecholamine-sensitive adenylate cyclase and demonstration of postsynaptic receptor localization in brain, *Proc. Natl. Acad. Sci. U.S.A.,* 80 (1983) 1840–1844.

61 Strader, C.D., Dixon, R.A.F., Cheung, A.H., Candelore, M.R., Blake, A.D. and Sigal, I.S., Mutations that uncouple the β-adrenergic receptor from G_s and increase agonist affinity, *J. Biol. Chem.,* 262 (1987) 16439–16443.

62 Strader, C.D., Sigal, I.S., Blake, A.D., Cheung, A.H., Register, R.B., Rands, E., Zemcik, B.A., Candelore, M.R. and Dixon, R.A.F., The carboxyl terminus of the hamster β-adrenergic receptor expressed in mouse L cells is not required for receptor sequestration, *Cell,* 49 (1987) 855–863.

63 Strader, C.D., Sigal, I.S., Register, R.B., Candelore, M.R., Rands, E. and Dixon, R.A.F., Identification of residues required for ligand binding to the β-adrenergic receptor, *Proc. Natl. Acad. Sci. U.S.A.,* 84 (1987) 4384–4388.

64 Torda, T., Yamaguchi, I., Hirata, F., Kopin, I. and Axelrod, J., Mepacrine treatment prevents immobilization-induced desensitization of beta-adrenergic receptors in rat hypothalamus and brainstem, *Brain Research,* 205 (1981) 441–444.

65 Tzagoloff, A., *Mitochondria,* Plenum, New York, 1982, 342 pp.

66 Verner, K. and Schatz, G., Protein translocation across membranes, *Science,* 241 (1988) 1307–1313.

67 Yarden, Y., Rodriguez, H., Wong, S.K.-F., Brandt, D.R., May, D.C., Burnier, J., Harkins, R.N., Chen, E.Y., Ramachandran, J., Ullrich, A. and Ross, E.M., The avian β-adrenergic receptor: primary structure and membrane topology, *Proc. Natl. Acad. Sci. U.S.A.,* 83 (1986) 6795–6799.

68 Young, D., Waitches, G., Birchmeier, C., Fasano, O. and Wigler, M., Isolation and characterization of a new cellular oncogene encoding a protein with multiple potential transmembrane domains, *Cell,* 45 (1986) 711–719.

69 Young III, W.S. and Kuhar, M.J., Noradrenergic α1 and α2 receptors: light microscopic autoradiographic localization, *Proc. Natl. Acad. Sci. U.S.A.,* 77 (1980) 1696–1700.

70 Zemcik, B.A. and Strader, C.D., Fluorescent localization of the β-adrenergic receptor on DDT-1 cells: down-regulation by adrenergic agonists, *Biochem. J.,* 251 (1988) 333–339.